Dynamic model updating using virtual antiresonances

Walter D'Ambrogio[a],[*] and Annalisa Fregolent[b]

[a]*Dipartimento di Energetica, Università de L'Aquila, Località Monteluco, I-67040 Roio Poggio (AQ), Italy*
[b]*Dipartimento di Meccanica e Aeronautica, Università di Roma "La Sapienza", Via Eudossiana 18, I-00184 Roma, Italy*

Questo lavoro è dedicato alla memoria di Bruno Piombo. Bruno era un nostro collega ed è stato tra i primi ad occuparsi, in Italia, di vibrazioni, analisi modale ed applicazioni alla meccanica di analisi del segnale. Ma ricordarlo solo come brillante professore e studioso non è sufficiente, perché Bruno era soprattutto un amico, una persona amabile che in tutte le occasioni di incontro si mostrava cortese e disponibile, evitando di far pesare il suo ruolo. Ci mancheranno il suo umorismo, che nascondeva a stento una profonda malinconia, la sua gentilezza e il suo modo di fare con i più giovani, quali noi eravamo nei suoi confronti. Questo modesto contributo è certamente un modo per ricordare Bruno a tutti coloro che gli volevano bene e lo stimavano, ma speriamo che serva anche per farlo conoscere a coloro che non hanno avuto l'opportunità di incontrarlo.

Abstract. This paper considers an extension of the model updating method that minimizes the antiresonance error, besides the natural frequency error. By defining virtual antiresonances, this extension allows the use of previously identified modal data. Virtual antiresonances can be evaluated from a truncated modal expansion, and do not correspond to any physical system. The method is applied to the Finite Element model updating of the GARTEUR benchmark, used within an European project on updating. Results are compared with those previously obtained by estimating actual antiresonances after computing low and high frequency residuals, and with results obtained by using the correlation (MAC) between identified and analytical mode shapes.

1. Introduction

The paper considers an extension of the model updating method that minimizes the antiresonance error [1], besides the natural frequency error. The location of antiresonant frequencies is a good correlation indicator between experimental and analytical frequency response functions (FRFs). Unlike natural frequencies, that are a global system property, antiresonant frequencies are typical of each FRF. In this sense, smartly chosen FRFs allow to add significant information. Furthermore, antiresonant frequencies are usually identified with much less error than mode shapes. Therefore, the use of antiresonance error in dynamic model updating may exhibit some advantages with respect to the more standard procedure based on mode shape error.

For the technique to provide its best performance, it is required to use antiresonant frequencies from point FRFs [1], i.e. when the excitation DoF and the response DoF are the same. However, modal testing usually involves measuring just a row or column of the FRF matrix (single reference modal testing), so that only one point FRF is available. Therefore, special testing procedures – to move the excitation DoF along with the response DoF – are required to apply this technique. If this is not allowed due to structure unavailability or to cost reasons, it would be necessary to obtain the antiresonant frequencies of the unmeasured point FRFs by other means. Such FRFs can be synthesized

---

[*]Corresponding author: Walter D'Ambrogio, Dipartimento di Energetica, Università de L'Aquila, Località Monteluco, I-67040 Roio Poggio (AQ), Italy. Tel.: +39 08624 34352; Fax: +39 08624 34303; E-mail: dambro@ing.univaq.it.

through a truncated expansion of identified modes, but this process may significantly affect the estimated location of antiresonant frequencies. This drawback can be avoided by using appropriate low and high frequency residuals accounting for the contribution of truncated modes [2].

Alternatively, the zeroes of the truncated expansion of the identified modes could be directly considered. Such zeroes will be defined as virtual antiresonances, because they do not correspond to any physical system. Obviously, the error on virtual antiresonances must be referred to the corresponding virtual antiresonances of the analytical model to be updated. The method is here applied to the GARTEUR testbed, a structure used as a benchmark in the EU sponsored COST ACTION F3 "Structural dynamics", within the Working Group 1: Dynamic model updating.

The results obtained by using virtual antiresonances are compared with those obtained in [2] by using low and high frequency residuals to estimate true antiresonances. A further comparison is made by using the correlation error, involving MAC between analytical and identified mode shapes. Since MAC and virtual antiresonances are computed using exactly the same piece of information, such comparison may highlight the effectiveness of the two quantities.

2. Updating technique

The following quantity is minimised for model updating. The first term is the weighted output residual, whilst the second term is a regularisation term used to limit the parameter variations:

$$\min_{\alpha} \mathbf{e}^T \mathbf{W} \mathbf{e} + \boldsymbol{\alpha}^T \mathbf{W}_\alpha \boldsymbol{\alpha} \tag{1}$$

Here $\mathbf{e} = \mathbf{y}_X - \mathbf{y}_A$ is the error (or residual) vector, $\mathbf{y}_X$ and $\mathbf{y}_A$ are the measured and the analytical output vectors, $\mathbf{W}$ is the error norm weighting matrix, $\boldsymbol{\alpha}$ contains the correction factors α_i and $\mathbf{W}_\alpha$ is the weighting matrix for the correction factor, defined as:

$$\alpha_i = \frac{(p_i)_{\text{upd.}} - (p_i)_{\text{init.}}}{(p_i)_{\text{init.}}} \tag{2}$$

where p_i are the model properties to be corrected and the subscripts $_{init.}$ and $_{upd.}$ refer to the initial and updated model.

Using the classical sensitivity approach, one obtains:

$$(\mathbf{S}^T \mathbf{W} \, \mathbf{S} + \mathbf{W}_\alpha) \boldsymbol{\alpha} = \mathbf{S}^T \mathbf{W} \mathbf{e} \tag{3}$$

where $\mathbf{S}$ is the sensitivity (or gradient) matrix of the output vector $\mathbf{y}_A$ to the model properties, or more precisely, to the correction factors $\boldsymbol{\alpha}$ ($S_{ij} = \partial y_{Ai}/\partial \alpha_j$), evaluated at a given linearisation point. The problem must be solved at each iteration step (k) for the actual linearisation point $\boldsymbol{\alpha}^{(k)}$. Numerical stability is enforced by limiting the step length, i.e.

$$\boldsymbol{\alpha}^{(k+1)} = \boldsymbol{\alpha}^{(k)} + \rho^{(k)} [(\mathbf{S}^T \mathbf{W} \mathbf{S} + \mathbf{W}_\alpha)^{(k)}]^+ \times \mathbf{S}^T \mathbf{W} \mathbf{e}^{(k)} \qquad k = 0, 1, \ldots \tag{4}$$

where $^+$ denotes the generalized inverse and $\rho^{(k)}$ is a step length control parameter ($\leqslant 1$) chosen to limit either the maximum component or the norm of $(\boldsymbol{\alpha}^{(k+1)} - \boldsymbol{\alpha}^{(k)})$.

2.1. Updating using antiresonant frequencies

A typical error vector could consist of natural frequency errors and mode shape errors. Natural frequencies can be identified quite accurately, but this does not hold for mode shapes. Therefore the feasibility of substituting mode shape amplitudes with antiresonant frequencies, that can be often identified much more accurately, was examined [1].

The considered error vector includes the natural frequencies f_{Xm}, $m = 1, \ldots, N_m$ and antiresonant frequencies z_{Xr}, $r = 1, \ldots, N_r$ both identified from several measured FRFs within a selected frequency range. The error vector $\mathbf{e}$, $(N_m + N_r) \times 1$, can be organised as:

$$\mathbf{e} = [\Delta f_1 \ldots \Delta f_{Nm} \quad \Delta z_1 \ldots \Delta z_{Nr}]^T \tag{5}$$

being $\Delta f_i = f_{Xi} - f_{Aj}$ and $\Delta z_i = z_{Xi} - z_{Aj}$, where f_{Aj} and z_{Aj} are the analytical natural frequencies and antiresonant frequencies that correspond to the identified ones f_{Xi} and z_{Xi}. For natural frequencies, the correspondence is established by using the Modal Assurance Criterion (MAC) whilst, for antiresonant frequencies, the correspondence is established by using the Frequency Domain Assurance Criterion (FDAC) [3]. Antiresonance sensitivities to model properties are provided in [1].

Since natural frequencies and antiresonant frequencies can be identified with similar amounts of error, it is not effective to use an error weighting matrix based on data inaccuracy. An error norm weighting matrix $\mathbf{W}$ can be introduced to normalize the error vector so that each term e_i is divided by the corresponding experimental quantity, thus providing the relative error ε_i. Therefore

$$\varepsilon_i = w_i e_i \qquad \text{or} \qquad \boldsymbol{\varepsilon} = \text{diag}(w_i)\mathbf{e} \tag{6}$$

where w_i are elements of the error weighting vector:

$$\mathbf{w} = \begin{pmatrix} f_{X_1}^{-1} \ldots f_{X_{Nm}}^{-1} & z_{X_1}^{-1} \ldots z_{X_{Nr}}^{-1} \end{pmatrix} \tag{7}$$

The error norm weighting matrix that corresponds to the previous error weighting vector is:

$$\mathbf{W} = \text{diag}\left(w_i^2\right) \tag{8}$$

In fact, the following equality must hold:

$$\mathbf{e}^T \mathbf{W} \mathbf{e} = \boldsymbol{\varepsilon}^T \boldsymbol{\varepsilon} = \mathbf{e}^T \text{diag}\left(w_i^2\right) \mathbf{e} \tag{9}$$

It was shown [1] that the technique is most effective when antiresonant frequencies are taken from point FRFs. In usual modal testing, only one drive point is available. Therefore special testing procedures, to move the excitation DOF along with the response DOF, would be required to obtain a set of point FRFs. Besides being more expensive, this prevents the use of previously obtained FRFs from single reference modal testing or previously identified modal parameters.

To use previously identified modal data, it is required to estimate antiresonant frequencies of unmeasured point FRFs. Such FRFs could be synthesized through truncated modal expansion, but modal truncation might seriously affect the location of antiresonances. To overcome this problem, one can try either to limit the deviation between the actual antiresonant frequencies and the synthesized ones, or to develop different quantities that, by definition, are not affected by modal truncation. The first approach consists in using appropriate low and high frequency residuals, the second one involves the definition of virtual antiresonances, i.e. the zeroes of a truncated modal expansion.

2.1.1. Antiresonant frequencies of synthesized point FRFs

Low and high frequency residuals account for the contribution of truncated modes. Such residuals are usually a byproduct of modal identification and are available only for measured FRFs. A possible theoretical estimation was proposed in [2]: it considers the contribution of rigid body and upper analytical modes. In the authors' experience, errors connected with this procedure can be usually accepted in this context. Undamped point inertances are therefore synthesized using the expression:

$$H_{rr}(f) = L_{rr} + \sum_{i=1}^{m} \frac{\phi_{Xri}^2}{1 - f_{Xi}^2/f^2} + \sum_{i=m+1}^{N} \frac{\phi_{Ari}^2}{1 - f_{Ai}^2/f^2} \tag{10}$$

where L_{rr} denotes the low frequency residual, the middle term is the contribution of identified modes ϕ_X and the last term is the high frequency residual estimated as the contribution of high frequency analytical modes ϕ_A. In many cases, the lower residual corresponds to the massline and can be computed using analytical rigid body modes.

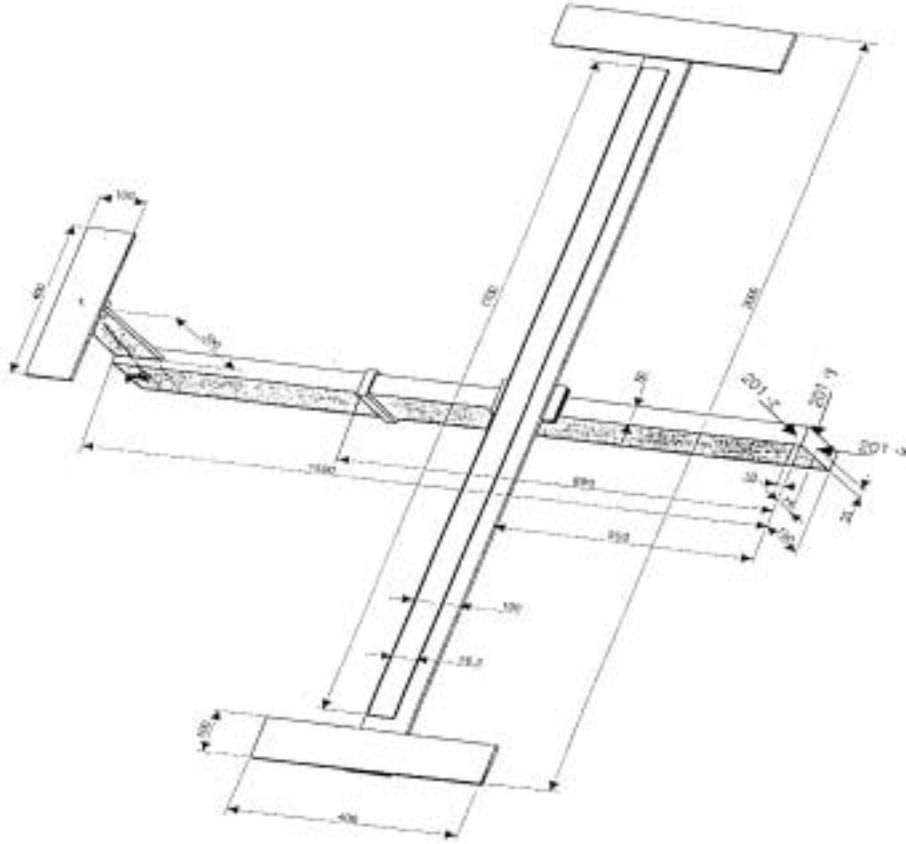Antiresonant frequencies are finally estimated by finding the zeroes of $H_{rr}(f)$.

Fig. 1. GARTEUR SM-AG19.

2.1.2. *Virtual antiresonances*

For a given FRF, virtual antiresonances can be defined as the zeroes of a truncated modal expansion, i.e. without low and high frequency residuals. Specifically, truncated point FRFs are considered. Their zeroes have no special physical significance, differently from true antiresonances, that correspond to natural frequencies of constrained systems. Hence the attribute of 'virtual' given to these quantities.

A truncated point FRF can be reduced to rational fraction polynomial form as follows:

$$H_{Trr}(f) = \sum_{i=1}^{N_m} \frac{\phi_{ri}^2}{1 - f_i^2/f^2} = \frac{\sum_{i=1}^{N_m} \phi_{ri}^2 \prod_{l=1,l\neq i}^{N_m} \left(1 - f_l^2/f^2\right)}{\prod_{i=1}^{N_m} \left(1 - f_i^2/f^2\right)} \tag{11}$$

Zeroes (virtual antiresonances) can be extracted from the numerator of Eq. (11), using identified and analytical modal parameters in turn. By using the identified modal parameters it is obtained:

$$\sum_{i=1}^{N_m} \phi_{Xri}^2 \prod_{l=1,l\neq i}^{N_m} \left(1 - f_{Xl}^2/f^2\right) = 0 \tag{12}$$

which can be solved numerically for the unknown frequencies and provides the test virtual antiresonances $\tilde{z}_{Xi}$, $i = 1, \ldots, N_m - 1$.

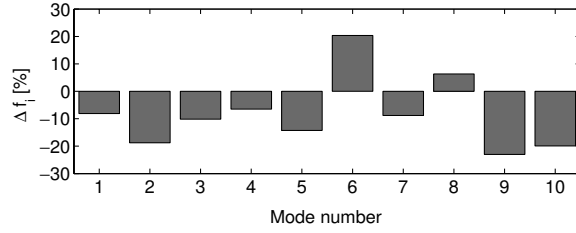By using the analytical modal parameters it is obtained:
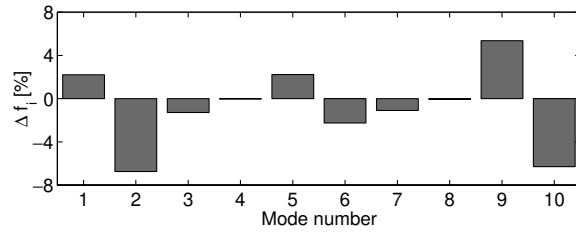
Fig. 2. Frequency deviations of the design model.

Fig. 3. Frequency deviations of the model updated from the design model.

$$\sum_{i=1}^{N_m} \phi_{Ari}^2 \prod_{l=1,l\neq i}^{N_m} \left(1 - f_{Al}^2/f^2\right) = 0 \tag{13}$$

which can be solved numerically for the unknown frequencies and provides the analytical virtual antiresonances $\tilde{z}_{Ai}$, $i = 1, \ldots, N_m - 1$.

In this case, errors on virtual antiresonances are considered instead of errors on true antiresonances. Then, the vector $\mathbf{e}$ becomes:

$$\mathbf{e} = [\Delta f_1 \ldots \Delta f_{Nm} \quad \Delta\tilde{z}_1 \ldots \Delta\tilde{z}_{Nr}]^T \tag{14}$$

being $\Delta\tilde{z}_i = \tilde{z}_{Xi} - \tilde{z}_{Aj}$, where $\tilde{z}_{Aj}$ are the virtual analytical antiresonant frequencies that correspond to the test ones $\tilde{z}_{Xi}$. In this case, the error weighting vector is:

$$\mathbf{w} = \left(f_{X_1}^{-1} \ldots f_{X_{Nm}}^{-1} \quad \tilde{z}_{X_1}^{-1} \ldots \tilde{z}_{X_{Nr}}^{-1}\right) \tag{15}$$

In this work, the sensitivities of virtual antiresonances to model properties $\partial\tilde{z}_{Ai}/\partial\alpha_j$ are evaluated numerically.

2.2. Updating using MAC

The results obtained by minimising the error on (virtual or true) antiresonances can be compared with those obtained by minimising the correlation (MAC) error between identified and analytical mode shapes. In this way, it is possible to observe the effectiveness of the two updating procedures, MAC and virtual antiresonances being evaluated by using the same piece of information.

The correlation (MAC) between identified and analytical modes is defined as:

$$\mathrm{MAC}(\phi_{Xi}, \phi_{Aj}) = \frac{|\phi_{Xi}^T \phi_{Aj}|^2}{(\phi_{Xi}^T \phi_{Xi})(\phi_{Aj}^T \phi_{Aj})} \tag{16}$$

In this case the error vector $\mathbf{e}$ includes the natural frequencies $f_{Xi}, i = 1, \ldots, N_m$ and the correlations, $\mathrm{MAC}(\phi_{Xi}, \phi_{Aj}), i = 1, \ldots, N_m$, between the experimental modes ϕ_{Xi} and the corresponding analytical modes ϕ_{Aj} in a given frequency range. The vector $\mathbf{e}$ becomes:

$$\mathbf{e} = [\Delta f_1 \ldots \Delta f_{Nm} \quad e_{\mathrm{MAC}_1} \ldots e_{\mathrm{MAC}_{Nm}}]^T \tag{17}$$

having defined the correlation error $e_{\mathrm{MAC}_i} = 1 - \mathrm{MAC}(\phi_{Xi}, \phi_{Aj})$.

Table 1
Model properties amenable to corrections

| Property	Symbol
Wings bending around longitudinal (X) axis	EI_x^w
Wings bending around vertical (Z) axis	EI_z^w
Wings torsion	GI_t^w
Wings mass density	ρA^w
Right winglet bending around transverse (Y) axis	EI_y^{rwt}
Left winglet bending around transverse (Y) axis	EI_y^{lwt}
Fuselage bending around transverse (Y) axis	EI_y^f
Fuselage bending around vertical (Z) axis	EI_z^f
Fuselage torsion	GI_t^f
Tail boom bending around longitudinal (X) axis	EI_x^{tb}
Tail boom torsion	GI_t^{tb}
Tail wing bending around longitudinal (X) axis	EI_x^{tw}
Fuselage-wing connection bending around longitudinal (X) axis	EI_x^{fwc}
Fuselage-wing connection torsion	GI_t^{fwc}
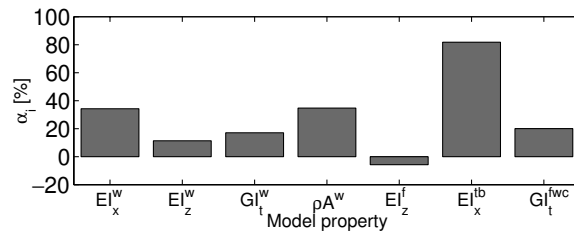
Fig. 4. Correction factors of the model updated from the design model.

The error weighting vector can be written as:

$$\mathbf{w} = \left(f_{X_1}^{-1} \ldots f_{X_{Nm}}^{-1} \quad w_1^{-1} \ldots w_{Nm}^{-1} \right) \tag{18}$$

where appropriately chosen w_i can be used to weight the MAC error with respect to the natural frequency error. For example, a typical choice could be to select such weights to be equal to 10. In fact, an acceptable MAC error can be about 10% whilst an acceptable natural frequency error is about 1%.

The MAC sensitivity to model properties is given by the following expression:

$$\frac{\partial}{\partial p_k} \text{MAC}(\phi_{Xi}, \phi_{Aj}) = \frac{2 \left[(\phi_{Xi}^T \phi_{Aj}) - (\phi_{Xi}^T \phi_{Xi})(\phi_{Xi}^T \phi_{Aj})^2 \phi_{Aj}^T \right]}{\left[(\phi_{Xi}^T \phi_{Xi})(\phi_{Aj}^T \phi_{Aj}) \right]^2} \times \frac{\partial \phi_{Aj}}{\partial p_k} \tag{19}$$

In this work, the derivatives $\partial \phi_{Aj}/\partial p_k$ are evaluated numerically.

3. Results

The structure used in these tests is the GARTEUR testbed shown in Fig. 1. It was built for a benchmark study on the European project COST ACTION F3 'Structural dynamics', in the working group 1 devoted to updating [4]. This structure represents a typical aircraft design with fuselage, wings and tail and it is described in [5,6]. The experimental FRFs and the identified modal data used in this work were made available for updating by London Imperial College [7].

3.1. Updating

Test data consist of FRFs measured in 24 locations with impact excitation from 0 to 70 Hz, and 10 normal modes. In the working group, it was agreed to use for updating only the frequency range up to 65 Hz (active frequency range
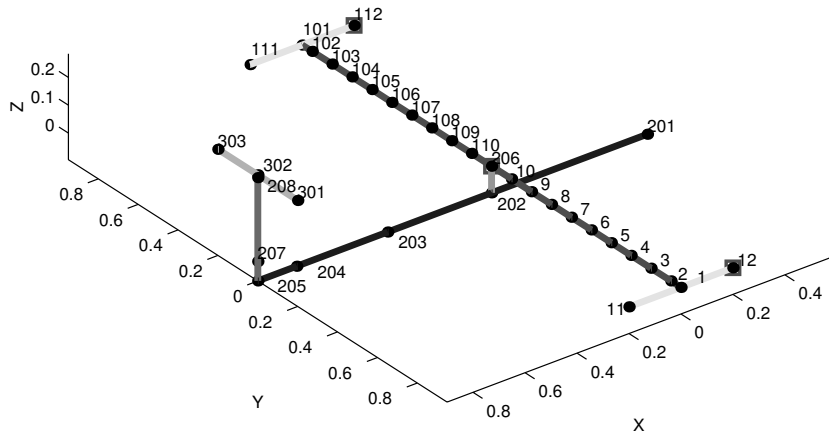
Fig. 5. Initial FE model of the GARTEUR SM-AG19 structure: 35 nodes (●), 34 beam elements, 3 lumped masses (■), 210 DOFs.
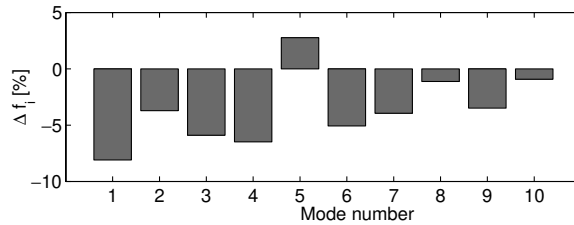

Fig. 6. Frequency deviation ($|\Delta f_{\mathrm{init}}| = 4.15\%$) of the initial model.

including modes from 1 to 9). The remaining mode is used to check the prediction of eigenfrequencies and modes beyond the active frequency range (passive frequencies).

In a first attempt, the model described as the design model in [5] was updated. The model has 32 beam elements, 33 nodes, 3 concentrated masses and 198 DOFs. The deviation between the FE design model and the experimental data is expressed by two quantities, the frequency deviation and the mode correlation, computed according to the definition suggested in [8]. For example, the frequency deviation of a single mode and its average over N_m modes are:

$$\Delta f_i = \frac{f_{Aj} - f_{Xi}}{f_{Xi}}; \quad |\Delta f| = \sum_{i=1}^{N_m} \frac{|\Delta f_i|}{N_m} \tag{20}$$

where f_{Xi} is the ith experimental natural frequency and f_{Aj} is the corresponding analytical eigenfrequency of the model.

Large frequency deviations of the design model are shown in Fig. 2. Updating is performed by minimizing natural frequency errors. Effective model properties are selected from the list in Table 1 after sensitivity analysis.

Figure 3 shows the frequency deviations of the updated model: they are still unsatisfactory, especially for modes 2 and 9. Correction factors are shown in Fig. 4: it is noticed that a very critical parameter is the tail boom bending stiffness.

Therefore, a finer discretisation of the tail boom is performed. Three beam elements are used instead of one: the two end elements are needed to better describe the joints between the tail boom and the fuselage and between the tail boom and the tail wing. The new 'initial' model is shown in Fig. 5.

The frequency deviation and mode correlation of the initial model, shown in Figs 6 and 7, respectively, are a much better starting point for updating. However, the need for updating is quite clear.

The initial model is updated by minimising three different error vectors: the first error vector contains the natural frequency errors of the active modes in combination with antiresonance errors of some FRF (R&A-updated model);
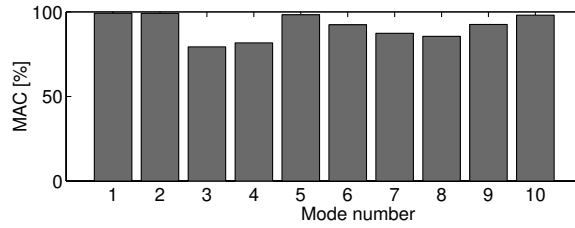
Fig. 7. Mode correlation of the initial model ($\overline{MAC}_{init} = 91.4\%$).
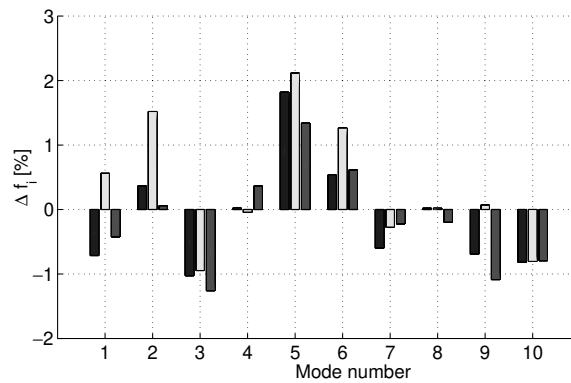

Fig. 8. Frequency deviation of the updated model: R&A dark gray, R&AV light gray, R&MAC medium gray.

the second one contains the natural frequency errors and the virtual antiresonance errors of the same FRFs (R&AV-updated model); the third one contains the natural frequency errors and the mode correlation (R&MAC-updated model). Hereafter, results related to the R&A-updated model will be displayed first in dark gray, those related to R&AV-updated model will be displayed in the middle in light gray whilst results of the R&MAC-updated model will appear last in medium gray.

Effective model properties are selected from the list in Table 1 after sensitivity analysis. Table 2 shows the sensitivity matrix of the active natural frequencies versus the model properties listed in Table 1. Although a low sensitivity does not imply that a parameter is not in error, trying to update low-sensitivity parameters may lead to large numerical errors. Therefore, parameters that can be updated are selected so that the ratio between the maximum in modulus sensitivity value in the matrix and the maximum sensitivity value in each column, corresponding to each parameter, is not greater than thirty. In Table 2, the maximum sensitivity value is highlighted in a box. Furthermore, the maximum sensitivity values of each column that comply with the previously stated criterion are underlined, whilst those not satisfying the criterion are shown in italic. The active resonances are significantly sensitive to 7 parameters only, but they are not sensitive to the tail wing bending stiffness, which should be considered an uncertain model property due to the joint between the tail boom and the tail wing. To increase the sensitivity to the tail wing bending stiffness, the antiresonances of the point FRF $H_{301Z,301Z}$ on the tail wing are also considered, together with mode correlation. Tables 3, 4 and 5 show the sensitivity matrices of antiresonances, virtual antiresonances and MAC versus the model properties, whose rows can be added in turn to the resonance sensitivity matrix of Table 2. The maximum sensitivity values of previously unsensitive parameters are underlined if they comply with the previously stated criterion, whilst they are shown in italic otherwise. Now the sensitivity to EI_x^{tw} is more significant. Consequently, 8 parameters, including the tail wing bending stiffness, can be effectively updated using the 9 natural frequencies of the active modes plus the antiresonances of $H_{301Z,301Z}$ in the active frequency range. It should be noted that MAC sensitivities could allow to try to update even more parameters but the choice will be restricted to only 8 parameters for comparison purposes.

Results of the model updating, obtained by minimising the three error vectors described previously, are summarised in Table 6. The frequency deviation is shown in Fig. 8. For the R&A-updated model, it is excellent for active modes (average value $|\Delta f_{act}| = 0.64\%$) and it is very good for passive modes ($|\Delta f_{pas}| = 0.82\%$). The frequency deviation

Table 2
Sensitivity matrix of natural frequencies to model properties

Mode	EI_x^w	EI_z^w	GI_t^w	ρA^w	EI_y^{rwt}	EI_y^{lwt}	EI_y^f	EI_z^f	GI_t^f	EI_x^{tb}	GI_t^{tb}	EI_x^{tw}	EI_x^{fwc}	GI_t^{fwc}
1	0.4588	0.0000	0.0005	−0.1178	0.0001	0.0001	0.0000	0.0000	0.0000	0.0000	0.0000	0.0000	0.0000	0.0000
2	0.3859	0.0009	0.0013	−0.0574	0.0002	0.0002	0.0000	0.0017	0.0051	0.0847	0.0000	0.0002	0.0009	0.0003
3	0.0151	0.0006	0.4182	−0.0395	0.0088	0.0088	0.0000	0.0011	0.0007	0.0170	0.0000	0.0001	0.0001	0.0002
4	0.0085	0.0000	0.4407	−0.0289	0.0091	0.0091	0.0002	0.0000	0.0000	0.0000	0.0000	0.0000	0.0000	0.0000
5	0.1946	0.0175	0.0346	−0.2347	0.0009	0.0009	0.0000	0.0259	0.0086	0.2238	0.0000	0.0013	0.0004	0.0053
6	0.4633	0.0001	0.0083	−0.3762	0.0013	0.0013	0.0003	0.0000	0.0000	0.0000	0.0000	0.0000	0.0000	0.0000
7	0.0387	0.2181	0.0005	−0.1210	0.0001	0.0001	0.0000	0.1382	0.0001	0.0174	0.0024	0.0008	0.0001	0.0638
8	0.0001	0.4934	0.0000	−0.1261	0.0000	0.0000	0.0005	0.0000	0.0000	0.0000	0.0000	0.0000	0.0000	0.0000
9	0.3218	0.0094	0.0008	−0.1914	0.0009	0.0009	0.0000	0.0089	0.0008	0.1297	0.0003	0.0054	0.0009	0.0025

Table 3
Sensitivity matrix of antiresonant frequencies to model properties

AR	EI_x^w	EI_z^w	GI_t^w	ρA^w	EI_y^{rwt}	EI_y^{lwt}	EI_y^f	EI_z^f	GI_t^f	EI_x^{tb}	GI_t^{tb}	EI_x^{tw}	EI_x^{fwc}	GI_t^{fwc}
1	0.1643	0.0000	0.0004	−0.0222	0.0000	0.0001	0.0001	0.0001	0.0044	0.2669	0.0000	0.0463	0.0006	0.0000
2	0.2924	0.0010	0.0061	−0.1369	0.0006	0.0004	0.0002	0.0014	0.0001	0.1100	0.0000	0.0562	0.0002	0.0003
3	0.0954	0.1387	0.0030	−0.1693	0.0002	0.0003	0.0001	0.1237	0.0069	0.0637	0.0007	0.0279	0.0005	0.0409
4	0.2610	0.0927	0.0020	−0.2162	0.0007	0.0007	0.0001	0.0497	0.0028	0.0290	0.0017	0.0240	0.0010	0.0269
5	0.0291	0.0385	0.0000	−0.0344	0.0003	0.0004	0.0004	0.3383	0.0003	0.0334	0.0044	0.0331	0.0001	0.0089

Table 4
Sensitivity matrix of virtual antiresonances to model properties

ARV	EI_x^w	EI_z^w	GI_t^w	ρA^w	EI_y^{rwt}	EI_y^{lwt}	EI_y^f	EI_z^f	GI_t^f	EI_x^{tb}	GI_t^{tb}	EI_x^{tw}	EI_x^{fwc}	GI_t^{fwc}
1	0.3211	−0.0037	0.0082	−0.1553	0.0008	0.0004	0.0000	−0.0036	−0.0022	0.1187	−0.0006	0.0186	0.0002	−0.0010
2	0.3714	0.0300	0.0021	−0.2463	0.0010	0.0009	0.0001	0.0104	0.0009	0.0327	0.0001	0.0111	0.0015	0.0070

Table 5
Sensitivity matrix of MAC to model properties

Mode	EI_x^w	EI_z^w	GI_t^w	ρA^w	EI_y^{rwt}	EI_y^{lwt}	EI_y^f	EI_z^f	GI_t^f	EI_x^{tb}	GI_t^{tb}	EI_x^{tw}	EI_x^{fwc}	GI_t^{fwc}
1	0.0015	−0.0000	−0.0023	0.2895	0.0004	0.0004	−0.0000	0.0000	−0.0000	0.0000	−0.0000	−0.0000	−0.0000	−0.0000
2	−0.1198	−0.0008	−0.0048	0.0975	0.0013	0.0007	0.0000	−0.0037	−0.0010	0.1250	0.0000	0.0039	−0.0007	−0.0002
3	−0.1547	−0.0090	0.3489	0.2474	0.1075	−0.0916	−0.0000	−0.0155	−0.0075	−0.1684	0.0000	−0.0004	−0.0005	−0.0027
4	−0.0539	0.0002	0.0486	0.0720	−0.0102	0.0191	0.0000	−0.0000	0.0000	−0.0000	−0.0000	0.0001	0.0000	−0.0000
5	0.5320	−0.0997	−0.8002	−0.2402	−0.0068	−0.0072	0.0000	−0.1178	0.0064	0.4999	0.0001	0.0201	0.0012	−0.0297
6	0.1348	−0.0072	−0.1511	0.2526	0.0108	0.0117	0.0006	0.0000	0.0000	0.0000	0.0000	0.0002	0.0000	0.0000
7	−0.5043	0.1377	−0.0256	0.5381	−0.0033	0.0031	−0.0000	0.3381	−0.0062	−0.1283	0.1211	0.0238	−0.0016	0.0451
8	−0.0236	−0.0024	0.0018	−0.0093	−0.0005	−0.0006	0.0121	−0.0000	0.0000	0.0000	0.0000	0.0045	0.0000	0.0000
9	0.1091	−0.1016	−0.0127	0.2553	0.0031	0.0088	0.0000	−0.0565	−0.0102	−0.0181	0.0141	0.0907	0.0016	−0.0274

of the R&AV-updated model is worse than in the previous case for active modes (average value $|\Delta f_{act}| = 0.76\%$) and very similar for passive modes ($|\Delta f_{pas}| = 0.80\%$). The frequency deviation of the R&MAC-updated model is excellent for active modes (average value $|\Delta f_{act}| = 0.62\%$) and very good for passive modes ($|\Delta f_{pas}| = 0.79\%$).

The mode correlation of the model updated by minimising the three error vectors described previously is shown in Fig. 9. The results are excellent in all the cases (see Table 6).

Figure 10 shows that the correction factors of the model updated by minimising the three error vectors described previously are very similar, except from the tail wing bending stiffness which shows a large correction only in the R&A case. In the R&AV case the correction is smaller whereas it is close to zero in the R&MAC case.

3.2. Validation of updating results

A way to validate the updated model is to check its capability to predict the dynamic behaviour of the original structure subjected to subsequent modifications. Two modifications were actually built: a first one, at the Imperial College (IC), consisting of a 0.95 kg mass added to the tail plane; a second one, at the University of Wales Swansea (UWS), consisting of a 0.724 kg mass added to the left drum [7].
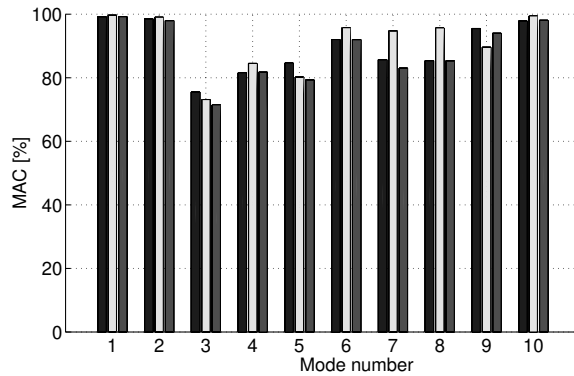
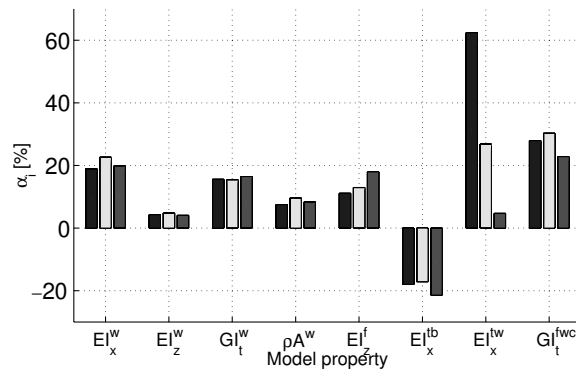Fig. 9. Mode correlation of the updated model: R&A dark gray, R&AV light gray, R&MAC medium gray.

Fig. 10. Correction factors of the updated model: R&A dark gray, R&AV light gray, R&MAC medium gray.

Table 6
Results of the model updating

Updated model	$|\Delta f_{\mathrm{act}}|$	$|\Delta f_{\mathrm{pas}}|$	$\overline{MAC}_{\mathrm{act}}$	$\overline{MAC}_{\mathrm{pas}}$
R&A residual	0.64%	0.82%	88.7%	97.9%
R&AV residual	0.76%	0.80%	90.3%	99.5%
R&MAC residual	0.62%	0.79%	87.1%	98.1%

The R&A-updated, R&AV-updated and R&MAC-updated models are used to predict the modal data of the structure subjected to the modifications 1 and 2 described previously. Results are summarised in Table 7.

The frequency deviation after modification 1 of the models updated by minimising the three residuals is shown in Fig. 11. The frequency deviation in the R&A and R&AV cases (average value over 11 modes: $|\Delta f| = 1.16\%$) is significantly better with respect to that of the R&MAC-updated model ($|\Delta f| = 1.91\%$). Note that although the average value of the frequency deviation is the same in the R&A and R&AV cases, in the R&AV case the frequency deviation of the first modes is lower than in the R&A case. Similar conclusions hold for mode correlation, shown in Fig. 12, which is very similar in the R&A and R&AV cases ($\overline{\mathrm{MAC}} = 93.1\%$ and $\overline{\mathrm{MAC}} = 92.7\%$, respectively) whereas it is significantly worse for modes 9 and 10 in the R&MAC case ($\overline{\mathrm{MAC}} = 88.7\%$).

The frequency deviation after modification 2 of the models updated by minimising the three residuals is shown in Fig. 13. The frequency deviation in the R&AV case (average value over 14 modes $|\Delta f| = 1.45\%$) is better with respect to that of the R&A-updated model ($|\Delta f| = 1.50\%$) and is significantly better with respect to the R&MAC case ($|\Delta f| = 1.67\%$). On the contrary, the mode correlation, shown in Fig. 14 is very similar in the three cases (see Table 7).
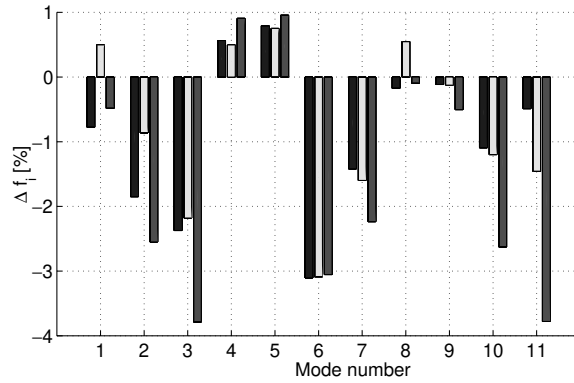
Fig. 11. Frequency deviation after modification 1 of the updated model: R&A dark gray, R&AV light gray, R&MAC medium gray.

Table 7
Results after modification 1 and 2

	Modification 1		Modification 2	
Updated model	$|\Delta f|$	$\overline{MAC}$	$|\Delta f|$	$\overline{MAC}$
R&A residual	1.16%	93.1%	1.50%	89.0%
R&AV residual	1.16%	92.7%	1.45%	88.9%
R&MAC residual	1.91%	88.7%	1.67%	88.1%
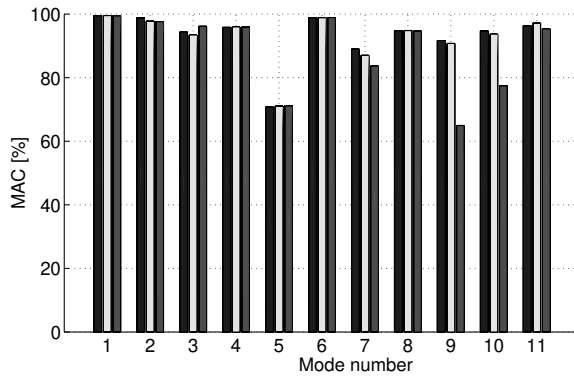
Fig. 12. Mode correlation after modification 1 of the updated model: R&A dark gray, R&AV light gray, R&MAC medium gray.

4. Conclusion

In this paper, an extension of the updating technique that minimises the error on virtual antiresonances, besides the natural frequency error, is considered. The technique is applied to the GARTEUR testbed. Results are compared to those obtained by different techniques that start with the same information (modal parameters).

In all cases, significant improvements of the frequency deviation are obtained starting from a very simple model (35 nodes, 34 beam elements, 210 DoFs). The best results are apparently those obtained by minimising the natural frequency error and the correlation error (R&MAC). Correction factors are very similar in the three cases, except from the tail wing bending stiffness which remains almost unchanged in the R&MAC case.

The subsequent validation is performed using results from modified structures. The results of the validation are acceptable in all cases, although the models updated by minimising the error on either true or virtual antiresonances prove to be much more accurate, especially in predicting the effect of modification 1, which is operated on the tail wing. It is clear that the tail wing bending stiffness requires the corrections obtained in the R&A and R&AV cases. This confirms that antiresonances – even virtual ones – may provide valuable information to the updating process. The advantage of antiresonances with respect to MAC is that antiresonances (from point FRFs) depend
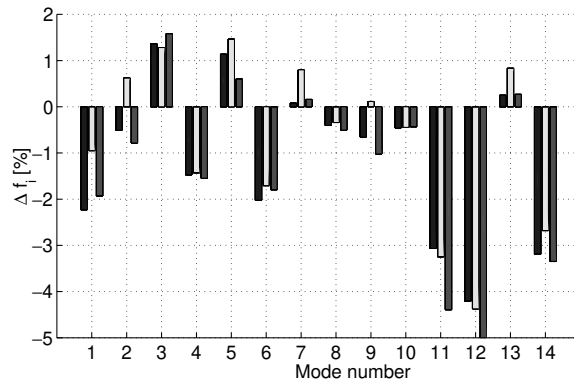
Fig. 13. Frequency deviation after modification 2 of the updated model: R&A dark gray, R&AV light gray, R&MAC medium gray.
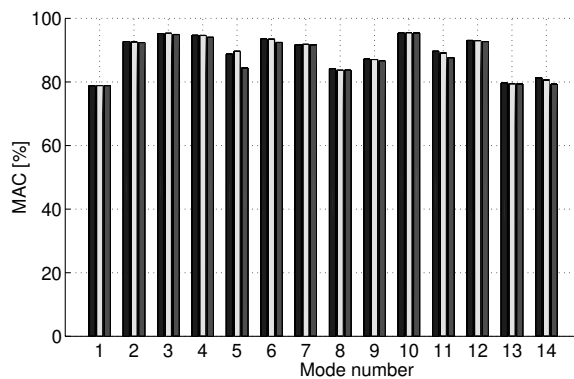

Fig. 14. Mode correlation after modification 2 of the updated model: R&A dark gray, R&AV light gray, R&MAC medium gray.

on mode shape amplitudes of all modes at a single DoF, whilst MAC is affected by mode shape amplitudes of a pair of correlated modes at all measured DoFs. Therefore, antiresonances can be more suited to correct local model properties.
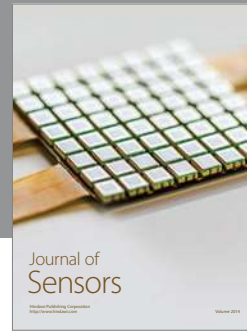
Acknowledgment

References

[1] W. D'Ambrogio and A. Fregolent, The Use Of Antiresonances For Robust Model Updating, *Journal of Sound and Vibration* **236** (2000), 227–243.

[2] W. D'Ambrogio and A. Fregolent, Results obtained by minimising natural frequency and antiresonance errors of a beam model, *Mechanical Systems and Signal Processing* **17** (2003), 29–37.

[3] R. Pascual, J.C. Golinval and M. Razeto, *A Frequency Domain Correlation Technique for Model Correlation and Updating*, 15th International Modal Analysis Conference, Orlando, USA, 1997, pp. 587–592.

[4] M. Link and M.I. Friswell, Working Group 1: Generation Of Validated Structural Dynamic Models – Results Of A Benchmark Study Utilising The Garteur Sm-Ag19 Test-Bed, *Mechanical Systems and Signal Processing* **17** (2003), 9–20.

[5] M. Degener and M. Hermes, *Ground Vibration Test and Finite Element Analysis of the GARTEUR SM-AG19 Testbed*, DLR, Göttingen, Germany, IB 232-96 J08, 1996.

[6]   M. Degener, *Ground Vibration Tests On An Aircraft Model Performed As Part Of A European Round Robin Excercise*, Forum on Aeroelasticity and Structural Dynamics, Rome, Italy, 1997, pp. 255–262.

[7]   M.I. Friswell, *New Measurements on the GARTEUR Testbed*, University of Wales Swansea, Swansea, U.K., 2000.

[8]   S. Keye, *Suggested Output Formats for the GARTEUR SM-AG19 Benchmark Results*, DLR, Göttingen, Germany, 1999.